Available online at www.sciencedirect.com
ScienceDirect
International Journal of Heat and Mass Transfer 51 (2008) 4002–4017
International Journal of HEAT and MASS TRANSFER
www.elsevier.com/locate/ijhmt

Finite circular fin method for wavy fin-and-tube heat exchangers under fully and partially wet surface conditions

Worachest Pirompugd [a,b], Chi-Chuan Wang [c], Somchai Wongwises [b,*]

[a] Department of Mechanical Engineering, Faculty of Engineering, Burapha University, Saensook, Muang, Chonburi 20131, Thailand
[b] Fluid Mechanics, Thermal Engineering and Multiphase Flow Research Lab. (FUTURE), Department of Mechanical Engineering, King Mongkut's University of Technology Thonburi, Bangmod, Bangkok 10140, Thailand
[c] Energy and Environment Research Laboratory, Industrial Technology Research Institute, Hsinchu, Taiwan 310, ROC

Received 4 May 2007; received in revised form 15 November 2007
Available online 5 March 2008

Abstract

The present study proposes the finite circular fin method for analyzing the heat and mass transfer characteristics of wavy fin-and-tube heat exchangers under fully and partially wet surface conditions. The analysis is carried out by dividing the wavy fin-and-tube heat exchanger into many tiny segments. The tiny segments can be analyzed based on surface conditions, i.e. fully wet, fully dry or partially wet surface condition. From the experimental results, it is found that the heat and mass transfer characteristics are insensitive to the inlet relative humidity but the effect of relative humidity on mass transfer characteristic become more pronounced when the partially wet surface condition takes place. The heat transfer characteristic is independent of the fin spacing. Effect of fin spacing on mass transfer characteristic is small when fin spacing is larger than 2.5 mm. However, at smaller fin spacing, the mass transfer characteristic slightly decreases when the relative humidity increases. The ratios of $h_{c,o}/h_{d,o}C_{p,a}$ are in the range of 0.6–1.2. Correlations are proposed to describe the heat and mass transfer characteristics. These correlations can describe 95.63% of the heat transfer characteristic within 15% and 95.14% of the mass transfer characteristic within 20%. Correspondingly, 94.68% of the ratios of $h_{c,o}/h_{d,o}C_{p,a}$ are predicted by the proposed correlation within 20%.
Published by Elsevier Ltd.

Keywords: Finite circular fin method; Fully dry surface condition; Fully wet surface condition; Heat transfer characteristic; Mass transfer characteristic; Partially wet surface condition; Wavy fin-and-tube heat exchangers

1. Introduction

The heat exchange process between two fluids that are at different temperature and separated by a solid wall may be found in air-conditioning, refrigeration, power production and many other thermal processing applications. The most widely used device used to implement the heat exchange process in association with the application of air-conditioning and refrigeration system is called a fin-and-tube heat exchanger which is actually an air-cooled heat exchanger with dominant resistance usually being in the air side. Hence enhanced surfaces are usually adopted for improving the overall heat transfer performance. Among the fin surfaces, the wavy fin-and-tube heat exchangers are one of the most popular fin surfaces applicable to both condenser and evaporator. In the evaporators, the temperatures of outside tube and fin surfaces are generally below the dew point temperature, leading to simultaneous heat and mass transfer outside tube and fin surfaces. In general, the complexity of the moist air flowing across the wavy fin-and-tube heat exchangers in dehumidifying conditions makes the theoretical simulations very difficult.

The air side performance of wavy fin-and-tube heat exchangers had been studied by many researchers (Beecher and Fagan [1], Yan and Sheen [2], Wang et al. [3–6], Lin

* Corresponding author. Tel.: +66 2 470 9115; fax: +66 2 470 9111.
E-mail address: somchai.won@kmutt.ac.th (S. Wongwises).

0017-9310/$ - see front matter Published by Elsevier Ltd.
doi:10.1016/j.ijheatmasstransfer.2007.11.049

Nomenclature

A_f	surface area of the fin, m^2
$A_{f,dry}$	surface area of fin of dry portion, m^2
$A_{f,wet}$	surface area of fin of wet portion, m^2
$A_{p,i}$	inside surface area of the tube, m^2
$A_{p,o}$	outside surface area of the tube, m^2
A_o	total surface area that is the summation of A_f and $A_{p,o}$, m^2
A_{wet}	outside surface area of wet portion, m^2
b'_p	slope of the saturated moist air enthalpy curved between the mean inside and outside tube surface temperatures, $J\ kg^{-1}\ K^{-1}$
b'_r	slope of the saturated moist air enthalpy curved between the mean water temperature and the mean inside tube surface temperature, $J\ kg^{-1}\ K^{-1}$
$b'_{w,f}$	slope of the saturated moist air enthalpy curved at the mean water film temperature of the fin surface, $J\ kg^{-1}\ K^{-1}$
$b'_{w,p}$	slope of the saturated moist air enthalpy curved at the mean water film temperature of the outside tube surface, $J\ kg^{-1}\ K^{-1}$
$C_{p,a}$	moist air specific heat at the constant pressure, $J\ kg^{-1}\ K^{-1}$
$C_{p,r}$	water specific heat at the constant pressure, $J\ kg^{-1}\ K^{-1}$
D_c	collar diameter, m
D_i	inside tube diameter, m
D_o	outside tube diameter, m
F	correction factor
F_p	fin pitch, m
f_r	water side friction factor
$G_{a,max}$	moist air maximum mass velocity based on the minimum flow area, $kg\ m^{-2}\ s^{-1}$
$h_{c,o}$	moist air side convection heat transfer coefficient, $W\ m^{-2}\ K^{-1}$
$h_{d,o}$	moist air side convection mass transfer coefficient, $kg\ m^{-2}\ s^{-1}$
h_r	water side convection heat transfer coefficient, $W\ m^{-2}\ K^{-1}$
I_0	modified Bessel function solution of the first kind, order 0
I_1	modified Bessel function solution of the first kind, order 1
i_a	moist air enthalpy, $J\ kg^{-1}$
$i_{a,in}$	inlet moist air enthalpy, $J\ kg^{-1}$
$i_{a,m}$	mean moist air enthalpy, $J\ kg^{-1}$
$i_{a,out}$	outlet moist air enthalpy, $J\ kg^{-1}$
i_g	saturated water vapor enthalpy, $J\ kg^{-1}$
$i_{s,f}$	saturated air enthalpy at the fin temperature, $J\ kg^{-1}$
$i_{s,f,b}$	saturated air enthalpy at the fin base temperature, $J\ kg^{-1}$
$i_{s,f,m}$	mean saturated air enthalpy at the mean fin surface temperature, $J\ kg^{-1}$
$i_{s,r,in}$	saturated air enthalpy at the inlet-water temperature, $J\ kg^{-1}$
$i_{s,r,m}$	mean saturated moist air enthalpy at the mean water temperature for the counter flow configuration, $J\ kg^{-1}$
$i_{s,r,out}$	saturated air enthalpy at the outlet-water temperature, $J\ kg^{-1}$
$i_{s,p,i,m}$	mean saturated air enthalpy at the mean inside tube wall temperature, $J\ kg^{-1}$
$i_{s,p,o,m}$	mean saturated air enthalpy at the mean outside tube wall temperature, $J\ kg^{-1}$
$i_{s,w}$	saturated air enthalpy at the water film temperature, $J\ kg^{-1}$
$i_{s,w,f,m}$	mean saturated air enthalpy at the mean water film temperature of the fin surface, $J\ kg^{-1}$
j_h	Colburn heat transfer group or Chilton–Colburn j-factor for the heat transfer
j_m	Colburn mass transfer group or Chilton–Colburn j-factor for the mass transfer
K_0	modified Bessel function solution of the second kind, order 0
K_1	modified Bessel function solution of the second kind, order 1
k_f	thermal conductivity of the fin, $W\ m^{-1}\ K^{-1}$
k_p	thermal conductivity of the tube, $W\ m^{-1}\ K^{-1}$
k_r	thermal conductivity of the water, $W\ m^{-1}\ K^{-1}$
k_w	thermal conductivity of the water film, $W\ m^{-1}\ K^{-1}$
L_p	tube length, m
$\dot{m}_a$	dry air mass flow rate, $kg\ s^{-1}$
$\dot{m}_r$	water mass flow rate, $kg\ s^{-1}$
N	number of tube row
P_d	wave height, m
P_l	longitudinal tube pitch, m
Pr_a	moist air side Prandtl number
Pr_r	water side Prandtl number
P_t	transverse tube pitch, m
$\dot{Q}_a$	moist air side heat transfer rate, W
$\dot{Q}_{avg}$	average heat transfer rate between the moist air and water sides, W
$\dot{Q}_{dry}$	heat transfer rate for fully dry segment, W
$\dot{Q}_{dry,conv,max}$	maximum heat transfer rate for dry portion in partially wet segment, W
$\dot{Q}_{part}$	heat transfer rate for partially wet segment, W
$\dot{Q}_{part,cond,r_i}$	heat transfer rate for partially wet segment evaluated at r_i, W
$\dot{Q}_r$	water side heat transfer rate, W
$\dot{Q}_{wet}$	heat transfer rate for a fully wet segment, W
$\dot{Q}_{wet,conv,max}$	maximum heat transfer rate for wet portion in partially wet segment, W
$\dot{Q}'_{wet,conv,max}$	maximum heat transfer rate for partially wet segment, W

R	ratio of the convection heat transfer characteristic to the convection mass transfer characteristic for the simultaneous convection heat and mass transfer
Re_{D_c}	moist air side Reynolds number based on the collar diameter
Re_{D_i}	water side Reynolds number
RH	inlet relative humidity of the moist air
r_i	inside fin radius for the equivalent circular area method that equal to the outside tube (include collar) radius, m
r_o	outside fin radius for the equivalent circular area method, m
r^*	distance from the center of the tube to the interface, m
Sc_a	moist air side Schmidt number
S_p	fin spacing, m
T_a	moist air temperature, K
$T_{a,in}$	inlet moist air temperature, K
$T_{a,m}$	mean moist air temperature for the counter flow configuration, K
$T_{a,out}$	outlet moist air temperature, K
T_{dp}	dew point temperature of the moist air, K
T_f	fin temperature, K
$T_{f,b}$	fin base temperature, K
$T_{f,t}$	fin tip temperature, K
$T_{f,m,cf}$	mean fin temperature for the counter flow configuration, K
$T_{p,i,m}$	mean inside tube surface temperature for the counter flow configuration, K
$T_{p,o,m}$	mean outside tube surface temperature for the counter flow configuration, K
$T_{r,m}$	mean water temperature for the counter flow configuration, K
T_r	water temperature, K
$T_{r,in}$	inlet-water temperature, K
$T_{r,out}$	outlet-water temperature, K
$T_{r,m}$	mean water temperature for the counter flow configuration, K
t	fin thickness, m
V_r	water velocity, m s^{-1}
$U_{o,d}$	overall heat transfer coefficient for fully dry surface condition, based on temperature difference, W m^{-2} T^{-1}
$U_{o,p}$	overall heat transfer coefficient for partially wet surface condition, based on enthalpy difference, kg m^{-2} s^{-1}
$U_{o,w}$	overall heat transfer coefficient for fully wet surface condition, based on enthalpy difference, kg m^{-2} s^{-1}
W_a	moist air humidity ratio
$W_{a,in}$	inlet moist air humidity ratio
$W_{a,m}$	mean moist air humidity ratio
$W_{a,out}$	outlet moist air humidity ratio
$W_{s,p,o,m}$	mean saturated air humidity ratio at the mean outside tube temperature
$W_{s,w}$	saturated air humidity ratio at the water film temperature
$W_{s,w,f,m}$	mean saturated air humidity ratio at the mean water film temperature at the fin surface
X_f	projected fin length, m
y_w	thickness of the water film, m
ρ_r	water density, kg m^{-3}
μ_r	viscosity of water, kg m^{-1} s^{-1}
$\eta_{f,dry}$	fully dry fin efficiency
$\eta_{f,part}$	partially wet fin efficiency
$\eta'_{f,part}$	effectively partially wet fin efficiency
$\eta_{f,wet}$	fully wet fin efficiency
θ_{dry,r^*}	air temperature difference at r^*, K
θ_{wet}	air enthalpy difference, kJ kg^{-1}
θ_{wet,r_i}	air enthalpy difference at r_i, kJ kg^{-1}
Δi_m	logarithmic mean enthalpy difference across the heat exchanger for the counter flow double-pipe configuration with the hot and cold fluid enthalpies, kJ kg^{-1}
ΔP	pressure difference, N m^{-2}
ΔT_m	logarithmic mean temperature difference across the heat exchanger for the counter flow double-pipe configuration with the hot and cold fluid temperatures, K

et al. [7], Pirompugd et al. [8,9]). Even though many efforts have been devoted to the study of wet-coils, the available literature on dehumidifying heat exchangers still offers limited information to assist the designer in sizing and rating a fin-and-tube heat exchanger. This can be made clear from the reported data which mainly focused on the study of the sensible heat transfer characteristics; very few attentions were paid to the mass transfer characteristics. Moreover, the fin surfaces may be fully wet, fully dry or partially wet depending on the difference between dew point temperature and surface temperature. Notice that if the outer tube surface (including collar) temperature is higher than the dew point temperature of moist air, there is only sensible heat transfer and is termed as fully dry condition. However, if the fin tip temperature is lower than the dew point temperature of moist air, both sensible and latent heat transfer occur at the same time for all fin surfaces. This condition is regarded as the fully wet condition. Occasionally, part of the fin tip temperature is higher than the dew point temperature whereas the rest of fin surface temperature is below the dew point temperature in such condition the partially wet surface prevails. There are few studies dealing with the heat transfer performance of the heat exchangers under partially wet surface conditions. Recently, Pirompugd et al. [9,10] presented the fully wet and fully dry tiny circular fin method for evaluation of heat and mass transfer characteristics under fully wet and partially wet surface conditions. Xia and Jacobi [11] formulated the logarithmic mean temperature difference (LMTD) and logarithmic mean enthalpy difference (LMED) methods for fully dry, fully wet, partially wet and frosted surface conditions. Pirompugd et al. [12] presented the new mathematical model namely "finite circular fin method (FCFM)" for the plain fin-and-tube heat exchangers under fully dry, fully wet and partially wet surface conditions. The FCFM characterizes by dividing a fin-and-tube heat exchanger into many tiny segments through which the detailed surface conditions (fully dry, fully wet, or partially wet surface) will be taken into account.

Although some information is currently available on the heat transfer performance of the heat exchangers under partially wet surface conditions, there still remains room for further work especially research on the mass transfer characteristics under partially wet surface condition. As a consequence, the objective of this study to provide a detailed method for analyzing the heat and mass transfer performances of fin-and-tube heat exchangers under partially wet surface conditions. The proposed method, namely the "finite circular fin method" (FCFM), is used to analyze the performance of the heat exchangers having wavy fin configuration under dehumidifying conditions.

2. Experimental apparatus

Fig. 1 shows the schematic diagram of the experimental apparatus. It consists of a closed-loop wind tunnel in which air is circulated by a centrifugal fan (7.46 kW, 10 HP) varying the air velocity with an inverter. The air duct is made from galvanized sheet steel and has an 850×550 mm cross-section. To obtain a uniform flow into the tested channel, air is forced through a mixer before entering the test section. The air flow is measured by multiple nozzles based on the ASHRAE Standard 41.2-1987 [13]. A differential pressure transducer is used to measure the pressure difference across the nozzles. The air temperatures at the inlet and exit zones across the sample heat exchangers are measured by two psychrometric boxes based on the ASHRAE Standard 41.1-1986 [14]. The dry-bulb and wet-bulb temperatures of the inlet-air are controlled by an air-ventilator that can provide a cooling capacity of up to 21.12 kW (6RT).

The working fluid in the tube side of the heat exchanger is chilled water. A thermostatically controlled reservoir provides cold water at selected temperatures. The temperature differences on the water side are measured by two pre-calibrated resistance temperature detectors (Pt – 100 Ω). The water volumetric flow rate is measured by a magnetic flow meter with a precision of ± 0.001 L s^{-1}. All the temperature measuring probes are resistance temperature devices, with a calibrated accuracy of ± 0.05 °C. In the experiments, only the data that satisfy the ASHRAE Standard 2000 [15] requirements (the energy balance condition, $\left|\dot{Q}_a - \dot{Q}_r\right| / \dot{Q}_{avg}$, is less than 0.05, where $\dot{Q}_r$ is the water side heat transfer rate, $\dot{Q}_a$ is the air side heat transfer rate and $\dot{Q}_{avg}$ is the average heat transfer rate between the air side and water side) are considered in the final analysis. A total of 18 wavy fin-and-tube heat exchangers, having various geometric parameters, are tested in this study. The details of test samples are shown in Table 1. The accuracies of the measurement sensors and the uncertainties in derived experimental values following the single-sample analysis proposed by Moffat [16], are given in Table 2. The geometric details of the tested wavy fins are shown in Fig. 2. The test fin-and-tube heat exchangers are tension wrapped having a "L" type fin collar. The test conditions approximate those encountered with typical fan-coils and evaporators of air-conditioning applications.

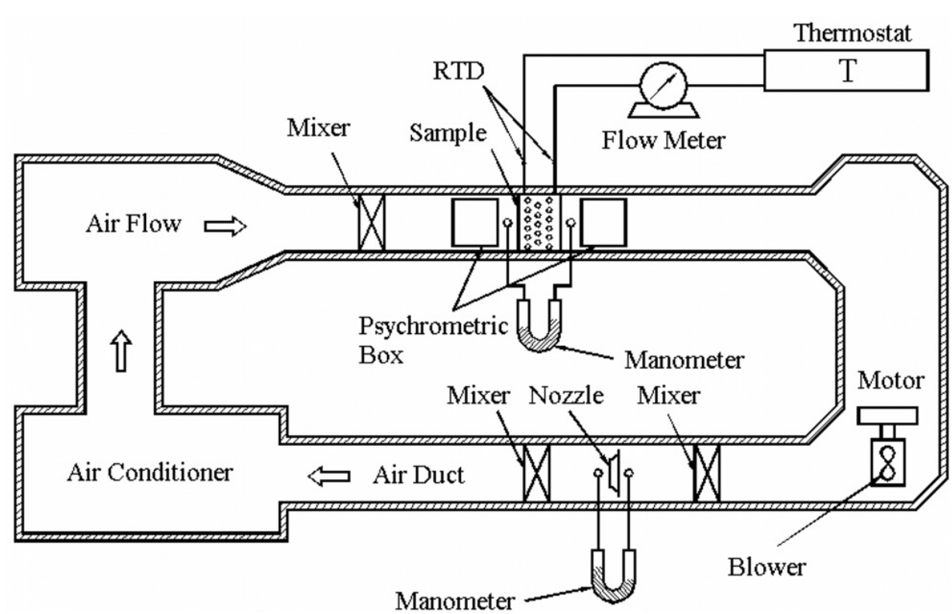

Fig. 1. Schematic diagram of experimental apparatus.

Table 1
Geometric dimensions of the sample wavy fin-and-tube heat exchangers

No.	F_p (mm)	S_p (mm)	t (mm)	D_c (mm)	P_t (mm)	P_l (mm)	P_d (mm)	X_f (mm)	N
1	1.60	1.48	0.12	10.38	25.4	19.05	1.18	4.7625	1
2	1.64	1.52	0.12	8.62	25.4	19.05	1.58	4.7625	1
3	2.82	2.70	0.12	10.38	25.4	19.05	1.18	4.7625	1
4	2.92	2.80	0.12	8.62	25.4	19.05	1.58	4.7625	1
5	3.54	3.42	0.12	8.62	25.4	19.05	1.58	4.7625	1
6	3.63	3.51	0.12	8.62	25.4	25.40	1.68	6.3500	1
7	1.69	1.57	0.12	8.62	25.4	19.05	1.18	4.7625	2
8	1.71	1.59	0.12	8.62	25.4	19.05	1.58	4.7625	2
9	3.12	3.00	0.12	8.62	25.4	19.05	1.58	4.7625	2
10	3.17	3.05	0.12	8.62	25.4	19.05	1.18	4.7625	2
11	1.64	1.52	0.12	8.62	25.4	19.05	1.58	4.7625	4
12	1.70	1.58	0.12	8.62	25.4	19.05	1.18	4.7625	4
13	3.07	2.95	0.12	8.62	25.4	19.05	1.58	4.7625	4
14	3.14	3.02	0.12	8.62	25.4	19.05	1.18	4.7625	4
15	1.57	1.45	0.12	10.38	25.4	19.05	1.18	4.7625	6
16	1.65	1.53	0.12	8.62	25.4	19.05	1.58	4.7625	6
17	2.82	2.70	0.12	10.38	25.4	19.05	1.18	4.7625	6
18	3.06	2.94	0.12	8.62	25.4	19.05	1.58	4.7625	6

Table 2
Summary of estimated uncertainties

Primary measurements		Derived quantities		
Parameter	Uncertainty	Parameter	Uncertainty $Re_{D_c} = 400$	Uncertainty $Re_{D_c} = 5000$
$\dot{m}_a$	0.3–1%	Re_{D_c}	±1.0%	±0.57%
$\dot{m}_r$	0.5%	$\dot{Q}_r$	±3.95%	±1.22%
ΔP	0.5%	$\dot{Q}_a$	±5.5%	±2.4%
T_r	0.05°C	j_h, j_m	±11.4%	±5.9%
T_a	0.1°C			

The test conditions of the inlet-air are as follows:

Dry-bulb temperature of the air 27 ± 0.5 °C
Inlet relative humidity for the incoming air 50% and 90%
Inlet-air velocity from 0.3 to 4.5 m s^{-1}
Inlet-water temperature 7 ± 0.5 °C
Water velocity inside the tube $1.5 \sim 1.7$ m s^{-1}

3. Mathematical model

The total heat transfer rate used in the calculation is the average of $\dot{Q}_a$ and $\dot{Q}_r$, namely:

$$\dot{Q}_a = \dot{m}_a(i_{a,in} - i_{a,out}) \tag{1}$$

$$\dot{Q}_r = \dot{m}_r C_{p,r}(T_{r,out} - T_{r,in}) \tag{2}$$

$$\dot{Q}_{avg} = \frac{\dot{Q}_a + \dot{Q}_r}{2} \tag{3}$$

In this study, a reduction method, namely the "finite circular fin method (FCFM)" published in our previous literature (Pirompugd et al. [12]) is used for detailed evaluation of the performance of wavy fin-and-tube heat exchanger instead of conventional lump approach. The proposed method is capable of handling test results for fully dry, fully wet and partially wet surface conditions. Analysis of the fin-and-tube heat exchanger is firstly carried out by dividing the heat exchanger into many tiny segments

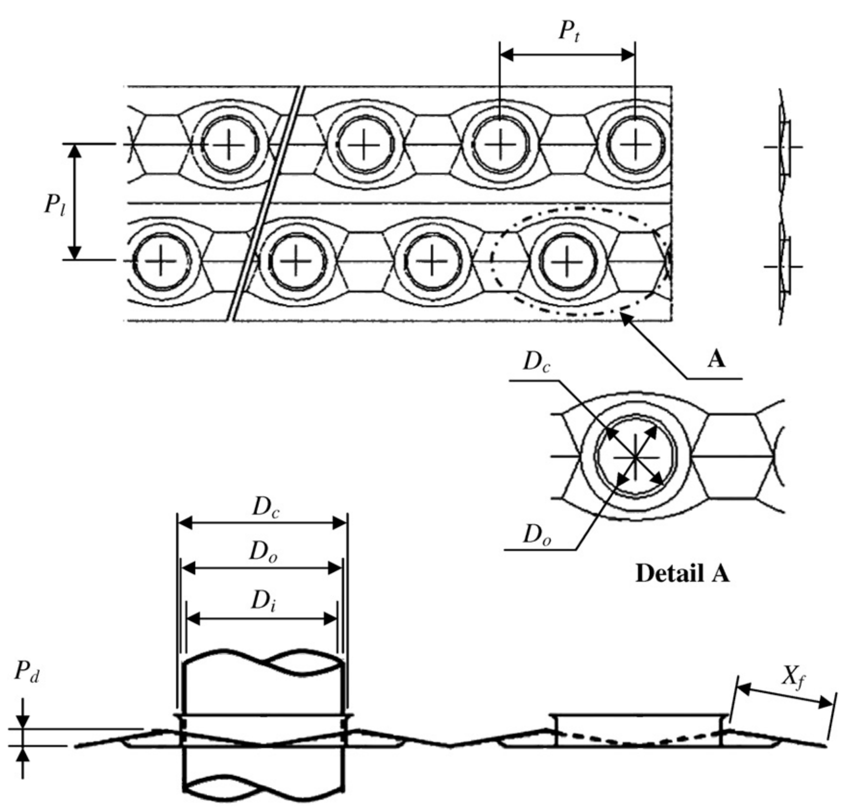

Fig. 2. Geometric detail of the herringbone wavy fin.

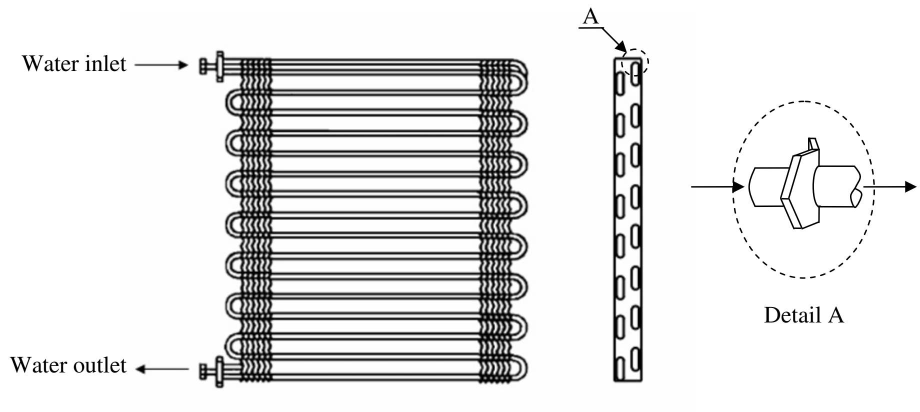

(a) Dividing the wavy fin-and-tube heat exchangers into may tiny segments

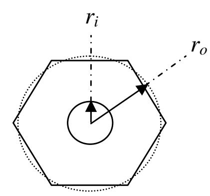

(b) Equivalent circular area method

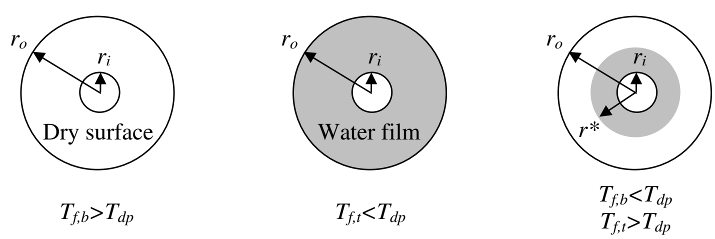

(c.1) Fully dry condition (c.2) Fully wet condition (c.3) Partially wet condition

(c) Circular fin in fully dry, fully wet and partially wet conditions

Fig. 3. Finite circular fin method (FCFM).

(number of tube rows × number of tube passes per row × number of fins) as shown in Fig. 3a. For calculation of the fin efficiency, the equivalent circular area method as shown in Fig. 3b is adopted. Depending on the surface condition, different reduction method is employed to the tiny segments. For fully dry condition, as shown in Fig. 3c.1, in which the outside tube (including collar) temperature is higher than the dew point temperature of the moist air, only sensible heat transfer occurs on the whole area of this tiny segment. The second case is the fully wet condition, as shown in Fig 3c.2, in which the fin tip temperature is lower than the dew point temperature of moist air. Both sensible and latent heat transfer takes place along every tiny segment. The last one is the partially wet condition, as shown in Fig. 3c.3, in which the outside tube (including collar) temperature is lower than the dew point temperature of the moist air but the fin tip temperature is opposite to that. Therefore in the region of $r_{\mathrm{i}} \leqslant r \leqslant r^*$ fully wet condition prevails whereas it is fully dry in the region of $r^* \leqslant r \leqslant r_{\mathrm{o}}$. In this study, we had proposed a reduction method that can resolve these three cases.

3.1. Tiny circular fin under partially wet condition

3.1.1. Heat transfer

The overall heat transfer coefficient, $U_{\mathrm{o,p}}$, is based on the enthalpy potential and is given as follows:

$$\dot{Q}_{\mathrm{part}} = U_{\mathrm{o,p}} A_{\mathrm{o}} \Delta i_{\mathrm{m}} F \tag{4}$$

where Δi_{m} is the mean enthalpy difference for a counter flow coil:

$$\Delta i_{\mathrm{m}} = i_{\mathrm{a,m}} - i_{\mathrm{s,r,m}} \tag{5}$$

According to Bump [17] and Myers [18], for the counter flow configuration, the mean enthalpy is

$$i_{\mathrm{a,m}} = i_{\mathrm{a,in}} + \frac{i_{\mathrm{a,in}} - i_{\mathrm{a,out}}}{\ln\left(\frac{i_{\mathrm{a,in}} - i_{\mathrm{s,r,out}}}{i_{\mathrm{a,out}} - i_{\mathrm{s,r,in}}}\right)} - \frac{(i_{\mathrm{a,in}} - i_{\mathrm{a,out}})(i_{\mathrm{a,in}} - i_{\mathrm{s,r,out}})}{(i_{\mathrm{a,in}} - i_{\mathrm{s,r,out}}) - (i_{\mathrm{a,out}} - i_{\mathrm{s,r,in}})} \tag{6}$$

$$i_{s,r,m} = i_{s,r,out} + \frac{i_{s,r,out} - i_{s,r,in}}{\ln\left(\frac{i_{a,in} - i_{s,r,out}}{i_{a,out} - i_{s,r,in}}\right)} - \frac{(i_{s,r,out} - i_{s,r,in})(i_{a,in} - i_{s,r,out})}{(i_{a,in} - i_{s,r,out}) - (i_{a,out} - i_{s,r,in})} \tag{7}$$

For the FCFM, F is the correction factor accounting for a single-pass, cross-flow heat exchanger for one fluid mixed, the other fluid being unmixed, as described by Threlkeld [19]. The overall heat transfer coefficient is related to the individual heat transfer resistance as follows:

$$\frac{1}{U_{o,p}} = \frac{b'_r A_o}{h_r A_{p,i}} + \frac{b'_p A_o \ln\left(\frac{D_c}{D_i}\right)}{2\pi k_p L_p} + \frac{1}{h_{o,w}\left(\frac{A_{p,o}}{b'_{w,p} A_o} + \frac{A_f \eta'_{f,part}}{b'_{w,f} A_o}\right)} \tag{8}$$

where

$$h_{o,w} = \frac{1}{\frac{C_{p,a}}{b'_{w,f} h_{c,o}} + \frac{y_w}{k_w}} \tag{9}$$

y_w in Eq. (9) is the thickness of the water film. A constant of 0.005 in. was proposed by Myers [18]. The water side heat transfer coefficient, h_r is evaluated from the Gnielinski correlation [20]:

$$h_r = \frac{(f_r/2)(Re_{D_i} - 1000)Pr_r}{1.07 + 12.7\sqrt{f_r/2}(Pr_r^{2/3} - 1)} \cdot \frac{k_r}{D_i} \tag{10}$$

and the friction factor, f_r is

$$f_r = \frac{1}{(1.58 \ln Re_{D_i} - 3.28)^2} \tag{11}$$

The Reynolds number used in Eqs. (10) and (11) is determined from $Re_{D_i} = \rho_r V_r D_i / \mu_r$. It is based on the inside diameter of the tube. In Eq. (8) there are four quantities (b'_r, b'_p, $b'_{w,p}$ and $b'_{w,f}$) involving enthalpy–temperature ratios that must be evaluated. The quantities of b'_r and b'_p can be calculated as

$$b'_r = \frac{i_{s,p,i,m} - i_{s,r,m}}{T_{p,i,m} - T_{r,m}} \tag{12}$$

$$b'_p = \frac{i_{s,p,o,m} - i_{s,p,i,m}}{T_{p,o,m} - T_{p,i,m}} \tag{13}$$

the values of $b'_{w,p}$ and $b'_{w,f}$ are the slopes of saturated enthalpy curves evaluated at the outer mean water film temperature at the base surface and the fin surface, respectively. Without loss of generality, $b'_{w,p}$ can be approximated by the slope of the saturated enthalpy curve evaluated at the base surface temperature (Wang et al. [21]). Evaluation of $b'_{w,f}$ requires a trial and error procedure. For the trial and error procedure, $i_{s,w,f,m}$ must be calculated using the following equation:

$$i_{s,w,f,m} \approx i_{a,m} - \frac{C_{p,a} h_{o,w} \eta'_{f,part}}{b'_{w,f} h_{c,o}} \times \left(1 - U_{o,p} A_o \left[\frac{b'_r}{h_r A_{p,i}} + \frac{b'_p \ln\left(\frac{D_c}{D_i}\right)}{2\pi k_p L_p}\right]\right) \times (i_{a,m} - i_{s,r,m}) \tag{14}$$

Hence, the corresponding fin efficiency is calculated by the equivalent circular area method as depicted in Fig. 3b. The partially wet fin efficiency (Pirompugd et al. [12]) can be written as

$$\eta_{f,part} = \frac{\dot{Q}_{part,cond,r_i}}{\dot{Q}_{wet,conv,max} + \dot{Q}_{dry,conv,max}} \tag{15}$$

where $\dot{Q}_{part,cond,r_i}$ is the heat transfer rate evaluated at r_i, $\dot{Q}_{wet,conv,max}$ is the convective heat transfer rate of wet portion that assumes the temperature of wet surface equal to fin base temperature whereas $\dot{Q}_{dry,conv,max}$ is the convective heat transfer rate of the dry portion that assumes the temperature of dry surface equal to the dry/wet interface temperature that is in fact equal to the dew point temperature. However, the partially wet fin efficiency obtained from Eq. (15) is not applicable for the Threlkeld's method. Because the heat transfer rate from Threlkeld's method is based on the enthalpy difference and cannot be directly applied to Eq. (15). In that respect, we had defined the effectively partially wet fin efficiency based on the enthalpy difference, and is given as

$$\eta'_{f,part} = \frac{\dot{Q}_{part,cond,r_i}}{\dot{Q}'_{wet,conv,max}} = \frac{\dot{Q}_{wet,conv,max} + \dot{Q}_{dry,conv,max}}{\dot{Q}'_{wet,conv,max}} \eta_{f,part} \tag{16}$$

where $\dot{Q}'_{wet,conv,max}$ is the convective heat transfer rate that assumes the temperature of all surface area equal to the fin base temperature. Then, the partially wet fin efficiency is

$$\eta_{f,part} = \frac{2r_i}{M_T(r*^2 - r_i^2)\theta_{wet,r_i} + M_T C_{p,a}\theta_{dry,r*}(r_o^2 - r*^2)} \times \left[\frac{\beta K_1(M_T r_i) - \alpha I_1(M_T r_i)}{M_T I_1(M_T r*) K_0(M_T r_i) + M_T I_0(M_T r_i) K_1(M_T r*)}\right] \tag{17}$$

where

$$\alpha = \theta_{wet,r_i} M_T K_1(M_T r*) + \gamma K_0(M_T r_i) \tag{18}$$

$$\beta = \theta_{wet,r_i} M_T I_1(M_T r*) - \gamma I_0(M_T r_i) \tag{19}$$

$$\gamma = b'_{w,f}\theta_{dry,r*} M_m \times \left[\frac{K_1(M_m r_o) I_1(M_m r*) - I_1(M_m r_o) K_1(M_m r*)}{K_1(M_m r_o) I_0(M_m r*) + I_1(M_m r_o) K_0(M_m r*)}\right] \tag{20}$$

$$M_T = \sqrt{\frac{2h_{o,w}}{k_{f}t}} \tag{21}$$

$$M_m = \sqrt{\frac{2h_{c,o}}{k_f t}} \tag{22}$$

θ_{wet,r_i} is the enthalpy difference evaluated at r_i and θ_{dry,r^*} is the temperature difference evaluated at r^*.

The corresponding partially wet fin efficiency is given as

$$\eta'_{\mathrm{f,part}} = \left(\frac{r*^2 - r_\mathrm{i}^2}{r_\mathrm{o}^2 - r_\mathrm{i}^2} + C_{\mathrm{p,a}}\frac{\theta_{\mathrm{dry},r*}}{\theta_{\mathrm{wet},r_\mathrm{i}}}\frac{r_\mathrm{o}^2 - r*^2}{r_\mathrm{o}^2 - r_\mathrm{i}^2}\right)\eta_{\mathrm{f,part}} \tag{23}$$

Eq. (17) can be applied to the fully wet condition by assigning r_o to r^*. An algorithm for calculation of the partially wet surface condition (Pirompugd et al. [12]) is given as follows:

1. Calculate the tube side heat transfer coefficient of h_r using Eq. (10).
2. Assume an outlet-air enthalpy of the calculated segment.
3. Calculate $i_{\mathrm{a,m}}$ by Eq. (6) and $i_{\mathrm{s,r,m}}$ by Eq. (7).
4. Assume values of $T_{\mathrm{p,i,m}}$ and $T_{\mathrm{p,o,m}}$.
5. Calculate $\frac{b'_\mathrm{r}A_\mathrm{o}}{h_\mathrm{r}A_{\mathrm{p,i}}}$ and $\frac{b'_\mathrm{p}A_\mathrm{o}\ln\left(\frac{D_\mathrm{c}}{D_\mathrm{i}}\right)}{2\pi k_\mathrm{p}L_\mathrm{p}}$.
6. Assume $T_{\mathrm{w,f,m}}$.
7. Assume r^*.
8. Calculate θ_{wet} at r^* from $\theta_{\mathrm{wet}} = \frac{\alpha I_0(M_\mathrm{T}r) + \beta K_0(M_\mathrm{T}r)}{M_\mathrm{T}I_1(M_\mathrm{T}r*)K_0(M_\mathrm{T}r_\mathrm{i}) + M_\mathrm{T}I_0(M_\mathrm{T}r_\mathrm{i})K_1(M_\mathrm{T}r*)}$.
9. Calculate $i_{\mathrm{s,f}}$ from θ_{wet} at r^*.
10. Calculate T_f from $i_{\mathrm{s,f}}$ at r^*.
11. If T_f obtained in step 10 is not equal to the dew point temperature of the moist air, the calculation steps 8–10 will be repeated with a new r^* until T_f is equal to the dew point temperature.
12. Calculate the $\eta_{\mathrm{f,part}}$ and $\eta'_{\mathrm{f,part}}$ using Eqs. (17) and (23), respectively.
13. Calculate $U_{\mathrm{o,p}}$ from Eq. (8).
14. Calculate $i_{\mathrm{s,w,f,m}}$ by Eq. (14).
15. Calculate $T_{\mathrm{w,f,m}}$ from $i_{\mathrm{s,w,f,m}}$.
16. If $T_{\mathrm{w,f,m}}$ obtained in step 15 is not equal to that assumed in step 6, the calculation steps 7–15 will be repeated with $T_{\mathrm{w,f,m}}$ obtained in step 15 until $T_{\mathrm{w,f,m}}$ is constant.
17. Calculate $\dot{Q}_{\mathrm{part}}$ from Eq. (4) of this segment.
18. Calculate $T_{\mathrm{p,i,m}}$ and $T_{\mathrm{p,o,m}}$ from the inside convection heat transfer rate and the conduction heat transfer rate.
19. If $T_{\mathrm{p,i,m}}$ and $T_{\mathrm{p,o,m}}$ obtained in step 18 are not equal to those assumed in step 4, the calculation steps 5–18 will be repeated with $T_{\mathrm{p,i,m}}$ and $T_{\mathrm{p,o,m}}$ obtained in step 18 until $T_{\mathrm{p,i,m}}$ and $T_{\mathrm{p,o,m}}$ are constant.
20. Calculate the outlet-air enthalpy and the outlet-water temperature from $\dot{Q}_{\mathrm{part}}$ obtained in step 17.
21. If the outlet-air enthalpy obtained in step 20 is not equal to that assumed in step 2, the calculation steps 3–20 will be repeated with the outlet-air enthalpy obtained in step 20 until the outlet-air enthalpy is constant.

3.1.2. Mass transfer

The cooling and dehumidifying of moist air by a cold surface involves simultaneously heat and mass transfer, and can be described by the process line equation from Threlkeld [19]:

$$\frac{\mathrm{d}i_\mathrm{a}}{\mathrm{d}W_\mathrm{a}} = R\frac{(i_\mathrm{a} - i_{\mathrm{s,w}})}{(W_\mathrm{a} - W_{\mathrm{s,w}})} + (i_\mathrm{g} - 2501R) \tag{24}$$

where R represents the ratio of heat transfer characteristic to mass transfer characteristic:

$$R = \frac{h_{\mathrm{c,o}}}{h_{\mathrm{d,o}}C_{\mathrm{p,a}}} \tag{25}$$

However, Eq. (25) did not correctly describe the dehumidification process on the psychrometric chart for the present fin-and-tube heat exchanger. This is because the saturated air enthalpy ($i_{\mathrm{s,w}}$) at the mean temperature of the fin surface is different from that at the fin base. In this regard, a modification of the process line on the psychrometric chart corresponding to the fin-and-tube heat exchanger is made. In this study, we had proposed a method to resolve the partially wet condition. From the energy balance of dehumidification process one can arrive at the following expression:

$$\begin{aligned}\dot{m}_\mathrm{a}\mathrm{d}i_\mathrm{a} = {} & \frac{h_{\mathrm{c,o}}}{C_{\mathrm{p,a}}}\mathrm{d}A_{\mathrm{p,o}}(i_{\mathrm{a,m}} - i_{\mathrm{s,p,o,m}}) + \frac{h_{\mathrm{c,o}}}{C_{\mathrm{p,a}}}\mathrm{d}A_{\mathrm{f,wet}}(i_{\mathrm{a,m}} - i_{\mathrm{s,w,f,m}}) \\ & + h_{\mathrm{c,o}}\mathrm{d}A_{\mathrm{f,dry}}(T_{\mathrm{a,m}} - T_{\mathrm{f,m}})\end{aligned} \tag{26}$$

Note that the first term on the right hand side denotes the heat transfer from the outside tube, the second term represents the heat transfer from wet part of the fin and the third term is the sensible heat transfer from dry part of fin. Conservation of mass of the water condensate leads to

$$\begin{aligned}\dot{m}_\mathrm{a}\mathrm{d}W_\mathrm{a} = {} & h_{\mathrm{d,o}}\mathrm{d}A_{\mathrm{p,o}}(W_{\mathrm{a,m}} - W_{\mathrm{s,p,o,m}}) \\ & + h_{\mathrm{d,o}}\mathrm{d}A_{\mathrm{f,wet}}(W_{\mathrm{a,m}} - W_{\mathrm{s,w,f,m}})\end{aligned} \tag{27}$$

Dviding Eq. (26) by Eq. (27) yields:

$$\frac{\mathrm{d}i_\mathrm{a}}{\mathrm{d}W_\mathrm{a}} = \frac{R\cdot(i_{\mathrm{a,m}} - i_{\mathrm{s,p,o,m}}) + R\cdot\left(\frac{r*^2 - r_\mathrm{i}^2}{r_\mathrm{o}^2 - r_\mathrm{i}^2}\right)\cdot(\varepsilon - 1)\cdot(i_{\mathrm{a,m}} - i_{\mathrm{s,w,f,m}}) + R\cdot\left(\frac{r_\mathrm{o}^2 - r*^2}{r_\mathrm{o}^2 - r_\mathrm{i}^2}\right)\cdot(\varepsilon - 1)\cdot C_\mathrm{p}(T_{\mathrm{a,m}} - T_{\mathrm{f,m}})}{(W_{\mathrm{a,m}} - W_{\mathrm{s,p,o,m}}) + \left(\frac{r*^2 - r_\mathrm{i}^2}{r_\mathrm{o}^2 - r_\mathrm{i}^2}\right)\cdot(\varepsilon - 1)\cdot(W_{\mathrm{a,m}} - W_{\mathrm{s,w,f,m}})} \tag{28}$$

where

$$\varepsilon = \frac{A_\mathrm{o}}{A_{\mathrm{p,o}}} \tag{29}$$

By assuming a value of R, Eq. (28) can be integrated. The mass transfer coefficient can be obtained accordingly. Procedures for obtaining the mass transfer coefficients for the partially wet condition are given in the following:

1. Obtain $W_{s,p,o,m}$ and $W_{s,w,f,m}$ from $i_{s,p,o,m}$ and $i_{s,w,f,m}$ from the calculations of heat transfer.
2. Assume a value of R.
3. Calculations are performed from the first element to the last element, employing the following procedures:
   3.1 Assume a humidity ratio at the exit of heat exchanger.
   3.2 Calculate the outlet humidity ratio of each element by Eq. (28).
   3.3 If the calculated outlet humidity ratio obtained from step 3.2 is not equal to the assumed value from step 3.1, repeat the calculation step 3.2.
4. If the calculated outlet-air humidity ratio for each element of the last row is not equal to the measured outlet-air humidity ratio, assume a new R value and repeat the calculation step 3 until the calculated outlet humidity ratio of the last row is equal to the measured outlet humidity ratio.

3.2. Tiny circular fin under fully wet condition

3.2.1. Heat transfer

Analogous to those reduction method for the foregoing partially wet condition, the overall heat transfer coefficient is based on the enthalpy potential and given as follows:

$$\dot{Q}_{\text{wet}} = U_{o,w}A_o\Delta i_m F \tag{30}$$

The overall heat transfer coefficient is related to the individual heat transfer resistances (Myers [18]) as follows:

$$\frac{1}{U_{o,w}} = \frac{b'_r A_o}{h_r A_{p,i}} + \frac{b'_p A_o \ln\left(\frac{D_c}{D_i}\right)}{2\pi k_p L_p} + \frac{1}{h_{o,w}\left(\frac{A_{p,o}}{b'_{w,p}A_o} + \frac{A_f \eta_{f,\text{wet}}}{b'_{w,f}A_o}\right)} \tag{31}$$

The quantities b'_r and b'_p can be calculated from Eqs. (12) and (13), respectively. The values of $b'_{w,p}$ and $b'_{w,f}$ are the slopes of saturated enthalpy curves evaluated at the outer mean water film temperature at the base surface and the fin surface, respectively. Without loss of generality, $b'_{w,p}$ can be approximated by the slope of the saturated enthalpy curve evaluated at the base surface temperature (Wang et al. [21]). Evaluation of $b'_{w,f}$ requires a trial and error procedure. For the trial and error procedure, $i_{s,w,f,m}$ must be calculated using the following equation:

$$i_{s,w,f,m} = i_{a,m} - \frac{C_{p,a}h_{o,w}\eta_{f,\text{wet}}}{b'_{w,f}h_{c,o}} \times \left(1 - U_{o,w}A_o\left[\frac{b'_r}{h_r A_{p,i}} + \frac{b'_p \ln\left(\frac{D_c}{D_i}\right)}{2\pi k_p L_p}\right]\right) \times (i_{a,m} - i_{s,r,m}) \tag{32}$$

The use of the enthalpy potential equation, greatly simplifies the fin efficiency calculation as illustrated by Kandlikar [22]. However, the original formulation of the wet fin efficiency by Threlkeld [19] was for straight fin configuration. For a circular fin, the wet fin efficiency is given by Wang, et al. [21] as follows:

$$\eta_{f,\text{wet}} = \frac{2r_i}{M_T(r_o^2 - r_i^2)}\left[\frac{K_1(M_T r_i)I_1(M_T r_o) - K_1(M_T r_o)I_1(M_T r_i)}{K_1(M_T r_o)I_0(M_T r_i) + K_0(M_T r_i)I_1(M_T r_o)}\right] \tag{33}$$

An algorithm for solving the heat transfer characteristic for the fully wet condition (Pirompugd et al. [8–10,23]) is given as follows:

1. Calculate the tube side heat transfer coefficient of h_r using Eq. (10).
2. Assume an outlet-air enthalpy of the calculated segment.
3. Calculate $i_{a,m}$ by Eq. (6) and $i_{s,r,m}$ by Eq. (7).
4. Assume values of $T_{p,i,m}$ and $T_{p,o,m}$.
5. Calculate $\frac{b'_r A_o}{h_r A_{p,i}}$ and $\frac{b'_p A_o \ln\left(\frac{D_c}{D_i}\right)}{2\pi k_p L_p}$.
6. Assume $T_{w,f,m}$.
7. Calculate the $\eta_{f,\text{wet}}$ using Eq. (33).
8. Calculate $U_{o,w}$ from Eq. (31).
9. Calculate $i_{s,w,f,m}$ by Eq. (32).
10. Calculate $T_{w,f,m}$ from $i_{s,w,f,m}$.
11. If $T_{w,f,m}$ obtained in step 10 is not equal to that assumed in step 6, the calculation steps 7–10 will be repeated with $T_{w,f,m}$ obtained in step 10 until $T_{w,f,m}$ is constant.
12. Calculate $\dot{Q}_{\text{wet}}$ from Eq. (30) of this segment.
13. Calculate $T_{p,i,m}$ and $T_{p,o,m}$ from the inside convection heat transfer rate and the conduction heat transfer rate.
14. If $T_{p,i,m}$ and $T_{p,o,m}$ obtained in step 13 are not equal to those assumed in step 4, the calculation steps 5–13 will be repeated with $T_{p,i,m}$ and $T_{p,o,m}$ obtained in step 13 until $T_{p,i,m}$ and $T_{p,o,m}$ are constant.
15. Calculate the outlet-air enthalpy and the outlet-water temperature from $\dot{Q}_{\text{wet}}$ obtained in step 12.
16. If the outlet-air enthalpy obtained in step 15 is not equal to that assumed in step 2, the calculation steps 3–15 will be repeated with the outlet-air enthalpy obtained in step 15 until the outlet-air enthalpy is constant.

3.2.2. Mass transfer

For the fully wet condition, the cooling and dehumidifying of the moist air by a cold surface involves the simultaneous heat and mass transfer and can be described by the process line equation (SI unit) from Threlkeld [19] as Eq. (24). However, for the present fin-and-tube heat exchanger, Eq. (24) did not directly describe the dehumidification process. This is because the saturated moist air enthalpy at the mean water film temperature on the fin surface is different from that at the outside tube surface. In this regard, a modification of the process line chart corresponding to the fin-and-tube heat exchangers is made. From the energy balance of the dehumidification, the rate equation can be arrived at the following expression:

$$\dot{m}_{\mathrm{a}} \mathrm{d} i_{\mathrm{a}}=\frac{h_{\mathrm{c,out}}}{C_{\mathrm{p,a}}} \mathrm{d} A_{\mathrm{p,out}}\left(i_{\mathrm{a,m}}-i_{\mathrm{s,p,o,m}}\right)+\frac{h_{\mathrm{c,out}}}{C_{\mathrm{p,a}}} \mathrm{d} A_{\mathrm{f}}\left(i_{\mathrm{a,m}}-i_{\mathrm{s,w,,f,m}}\right) \tag{34}$$

Note that the first term on the right hand side denotes the heat transfer of the outside tube whereas the second term is the heat transfer for the fin part. Conservation of the water condensate gives:

$$\begin{aligned}\dot{m}_{\mathrm{a}} \mathrm{d} W_{\mathrm{a}}= & h_{\mathrm{d,out}} \mathrm{d} A_{\mathrm{p,out}}\left(W_{\mathrm{a,m}}-W_{\mathrm{s,p,o,m}}\right) \\ & +h_{\mathrm{d,out}} \mathrm{d} A_{\mathrm{f}}\left(W_{\mathrm{a,m}}-W_{\mathrm{s,w,f,m}}\right)\end{aligned} \tag{35}$$

Dividing the equation of the heat transfer rate (Eq. (34)) by the equation of the mass transfer rate (Eq. (35)) yields:

$$\frac{\mathrm{d} i_{\mathrm{a}}}{\mathrm{d} W_{\mathrm{a}}}=\frac{R \cdot\left(i_{\mathrm{a,m}}-i_{\mathrm{s,p,o,m}}\right)+R \cdot(\varepsilon-1) \cdot\left(i_{\mathrm{a,m}}-i_{\mathrm{s,w,f,m}}\right)}{\left(W_{\mathrm{a,m}}-W_{\mathrm{s,p,o,m}}\right)+(\varepsilon-1) \cdot\left(W_{\mathrm{a,m}}-W_{\mathrm{s,w,f,m}}\right)} \tag{36}$$

By assuming a value of the ratio of heat transfer to mass transfer, R and by integrating Eq. (36), the moist air side convective mass transfer performance can be obtained. Procedures for obtaining the mass transfer coefficients for the partially wet condition are given in the following:

1. Obtain $W_{\mathrm{s,p,o,m}}$ and $W_{\mathrm{s,w,f,m}}$ from $i_{\mathrm{s,p,o,m}}$ and$i_{\mathrm{s,w,f,m}}$ from the calculations of heat transfer.
2. Assume a value of R.
3. Calculations are performed from the first element to the last element, employing the following procedures:
   3.1 Assume a humidity ratio at the exit of heat exchanger.
   3.2 Calculate the outlet humidity ratio of each element by Eq. (36).
   3.3 If the calculated outlet humidity ratio obtained from step 3.2 is not equal to the assumed value from step 3.1, repeat the calculation step 3.2.
4. If the calculated outlet-air humidity ratio for each element of the last row is not equal to the measured outlet-air humidity ratio, assume a new R value and repeat the calculation step 3 until the calculated outlet humidity ratio of the last row is equal to the measured outlet humidity ratio.

3.3. Tiny circular fin under fully dry condition

3.3.1. Heat transfer

For fully dry condition, the overall heat transfer coefficient based on the temperature difference is given as follows:

$$\dot{Q}_{\mathrm{dry}}=U_{\mathrm{o,d}} A_{\mathrm{o}} \Delta T_{\mathrm{m}} F \tag{37}$$

The term of $\Delta T_{\mathrm{m,cf}}$ can be shown as

$$\Delta T_{\mathrm{m}}=T_{\mathrm{a,m}}-T_{\mathrm{r,m}} \tag{38}$$

According to Bump [17], for the counter flow configuration, the mean temperature difference is

$$T_{\mathrm{a,m}}=T_{\mathrm{a,in}}+\frac{T_{\mathrm{a,in}}-T_{\mathrm{a,out}}}{\ln \left(\frac{T_{\mathrm{a,in}}-T_{\mathrm{r,out}}}{T_{\mathrm{a,out}}-T_{\mathrm{r,in}}}\right)}-\frac{\left(T_{\mathrm{a,in}}-T_{\mathrm{a,out}}\right)\left(T_{\mathrm{a,in}}-T_{\mathrm{r,out}}\right)}{\left(T_{\mathrm{a,in}}-T_{\mathrm{r,out}}\right)-\left(T_{\mathrm{a,out}}-T_{\mathrm{r,in}}\right)} \tag{39}$$

$$T_{\mathrm{r,m}}=T_{\mathrm{r,out}}+\frac{T_{\mathrm{r,out}}-T_{\mathrm{r,in}}}{\ln \left(\frac{T_{\mathrm{a,in}}-T_{\mathrm{r,out}}}{T_{\mathrm{a,out}}-T_{\mathrm{r,in}}}\right)}-\frac{\left(T_{\mathrm{r,out}}-T_{\mathrm{r,in}}\right)\left(T_{\mathrm{a,in}}-T_{\mathrm{r,out}}\right)}{\left(T_{\mathrm{a,in}}-T_{\mathrm{r,out}}\right)-\left(T_{\mathrm{a,out}}-T_{\mathrm{r,in}}\right)} \tag{40}$$

For the FCFM, F is the correction factor accounting for a single-pass, cross-flow heat exchanger for one fluid mixed, the other fluid being unmixed. The overall heat transfer coefficient is showed as follows:

$$\frac{1}{U_{\mathrm{o,d}}}=\frac{A_{\mathrm{o}}}{h_{\mathrm{r}} A_{\mathrm{p,i}}}+\frac{A_{\mathrm{o}} \ln \left(\frac{D_{\mathrm{c}}}{D_{\mathrm{i}}}\right)}{2 \pi k_{\mathrm{p}} L_{\mathrm{p}}}+\frac{1}{h_{\mathrm{c,o}}\left(\frac{A_{\mathrm{p,o}}}{A_{\mathrm{o}}}+\frac{A_{\mathrm{f}} \eta_{\mathrm{f,dry}}}{A_{\mathrm{o}}}\right)} \tag{41}$$

Kern and Kraus [24] determined the dry fin efficiency for a circular fin as follows:

$$\eta_{\mathrm{f,dry}}=\frac{2 r_{\mathrm{i}}}{M_{\mathrm{m}}\left(r_{\mathrm{o}}^{2}-r_{\mathrm{i}}^{2}\right)}\left[\frac{K_{1}\left(M_{\mathrm{m}} r_{\mathrm{i}}\right) I_{1}\left(M_{\mathrm{m}} r_{\mathrm{o}}\right)-K_{1}\left(M_{\mathrm{m}} r_{\mathrm{o}}\right) I_{1}\left(M_{\mathrm{m}} r_{\mathrm{i}}\right)}{K_{1}\left(M_{\mathrm{m}} r_{\mathrm{o}}\right) I_{0}\left(M_{\mathrm{m}} r_{\mathrm{i}}\right)+K_{0}\left(M_{\mathrm{m}} r_{\mathrm{i}}\right) I_{1}\left(M_{\mathrm{m}} r_{\mathrm{o}}\right)}\right] \tag{42}$$

An algorithm for solving the heat transfer characteristic for the fully dry condition (Pirompugd et al. [9,10]) is given as follows:

1. Calculate the tube side heat transfer coefficient of h_{r} using Eq. (10).
2. Assume an outlet-air temperature of the calculated segment.
3. Calculate $T_{\mathrm{a,m}}$ by Eq. (39) and $T_{\mathrm{r,m}}$ by Eq. (40).
4. Assume values of $T_{\mathrm{p,i,m}}$ and $T_{\mathrm{p,o,m}}$.
5. Calculate $\frac{b_{\mathrm{r}}' A_{\mathrm{o}}}{h_{\mathrm{r}} A_{\mathrm{p,i}}}$ and $\frac{b_{\mathrm{p}}' A_{\mathrm{o}} \ln \left(\frac{D_{\mathrm{c}}}{D_{\mathrm{i}}}\right)}{2 \pi k_{\mathrm{p}} L_{\mathrm{p}}}$.
6. Calculate the $\eta_{\mathrm{f,dry}}$ using Eq. (42).
7. Calculate $U_{\mathrm{o,d}}$ from Eq. (41).
8. Calculate $\dot{Q}_{\mathrm{dry}}$ from Eq. (37) of this segment.
9. Calculate $T_{\mathrm{p,i,m}}$ and $T_{\mathrm{p,o,m}}$ from the inside convection heat transfer rate and the conduction heat transfer rate.
10. If $T_{\mathrm{p,i,m}}$ and$T_{\mathrm{p,o,m}}$ obtained in step 9 are not equal to those assumed in step 4, the calculation steps 5–9 will be repeated with $T_{\mathrm{p,i,m}}$ and $T_{\mathrm{p,o,m}}$ obtained in step 9 until $T_{\mathrm{p,i,m}}$ and $T_{\mathrm{p,o,m}}$ are constant.
11. Calculate the outlet-air temperature and the outlet-water temperature from $\dot{Q}_{\mathrm{dry}}$ obtained in step 8.

12. If the outlet-air temperature obtained in step 11 is not equal to that assumed in step 2, the calculation steps 3–11 will be repeated with the outlet-air temperature obtained in step 11 until the outlet-air temperature is constant.

In this study, detailed evaluation algorithm of the heat transfer coefficient $h_{c,o}$ with the present FCFM relative to conventional lump approach is given as follows:

1. Calculate the moist air side heat transfer rate and the water side heat transfer rate by Eqs. (1) and (2), respectively.
2. Calculate the total heat transfer rate from Eq. (3).
3. Assume $h_{c,o}$ for all segments.
4. Calculate the heat transfer performance for each segment with the following procedures.
   4.1 Calculate the dew point temperature.
   4.2 Assign $T_{r,m}$ to $T_{p,i,m}$ and $T_{p,o,m}$.
   4.3 Calculate the fin tip temperature for the fully wet condition from $\theta_{\text{wet}} = \frac{\alpha I_0(M_T r)+\beta K_0(M_T r)}{M_T I_1(M_T r*)K_0(M_T r_i)+M_T I_0(M_T r_i)K_1(M_T r*)}$ by assigning r_o to r^*.
   4.4 If $T_{p,o,m}$ is higher than the dew point temperature, the algorithm of the fully dry condition is done.
   4.5 If the fin tip temperature is lower than the dew point temperature, the algorithm of the fully wet condition is adopted.
   4.6 If $T_{p,o,m}$ is lower than the dew point temperature but the fin tip temperature is higher than the dew point temperature, the algorithm of the partially wet condition is used.
   4.7 If $T_{p,i,m}$ and $T_{p,o,m}$ obtained in step 4.4–4.6 are not equal to those assumed in step 4.2, the calculation steps 4.3–4.6 will be repeated with $T_{p,i,m}$ and $T_{p,o,m}$ obtained in step 4.4–4.6 until $T_{p,i,m}$ and $T_{p,o,m}$ are constant.
5. If the summation of the heat transfer rate for all elements is not equal to the total heat transfer rate obtained in step 2, $h_{c,o}$ will be assumed with a new value and the calculation step 4 will be repeated until the summation of the heat transfer rate for all elements is equal to the total heat transfer rate.

The FCFM also provides a detailed evaluation of the performance of fin-and-tube heat exchanger that is superior to the conventional lump approach. An algorithm for solving the mass coefficient $h_{d,o}$ is given as follows:

1. If $T_{p,o,m}$ is higher than the dew point temperature, The outlet humidity ratio is equal to the inlet humidity ratio.
2. If the fin tip temperature is lower than the dew point temperature, the algorithm of the fully wet condition is employed.
3. If $T_{p,o,m}$ is lower than the dew point temperature but the fin tip temperature is higher than the dew point temperature, the algorithm of the partially wet condition is done.

3.4. Chilton–Colburn j-factor for heat and mass transfer (j_h and j_m)

The reduced results of the heat and mass transfer characteristics are in terms of dimensionless groups:

$$j_h = \frac{h_{c,o}}{G_{a,max} C_{p,a}} Pr_a^{2/3} \tag{43}$$

$$j_m = \frac{h_{d,o}}{G_{a,max}} Sc_a^{2/3} \tag{44}$$

4. Results and discussion

The j_h and j_m is the dimensionless parameters representing the heat and mass characteristics, respectively. The results by FCFM are compared with those by the original Threlkeld method, and are shown in Fig. 4a and b. For the heat transfer characteristic, Fig. 4a show the agreement of 97.67% of j_h between those obtained by the original Threlkeld method and those obtained by the present FCFM falls within −15% to 30%. However, j_m obtained by the FCFM is not consistent with those obtained by the Threlkeld method. The major deviation is because that the Threlkeld method is applicable to the fully wet surface only. Hence from the comparison one can see the major deviations are mainly pertaining to the partially wet surface. In addition, the mass transfer characteristic obtained from the original process line approach derived by the Threlkeld based on pure counter flow arrangements. For comparison with the fully wet and fully dry tiny circular fin method proposed by Pirompugd et al. [9,10], as shown in Fig. 5a and b, the j_h and j_m for fully wet condition obtained by the present method is identical to those obtained by the previous method. However, for the partially wet conditions, a noticeable difference occurs between those obtained by the present method and the previous method. This can be describe that the tiny segments for FCFM can take care of all surface conditions (including the tiny segments with the partially wet condition) but the tiny segment for the previous method (fully wet and fully dry tiny circular fin method) can manage only either fully dry or fully wet surface condition.

Fig. 6a–d show the influences of inlet relative humidity and of fin spacing on the heat transfer characteristics. When $500 < Re_{D_c} < 5000$ and $2 \leqslant N \leqslant 4$, the j_h are insensitive to change of the inlet relative humidity. However, when $Re_{D_c} < 500$, a level-off for j_h is encountered. This is in connection with the condensate retention phenomenon at very low Reynolds number region, in this situation the water condensed is easily hanging between the fin spacing and give rise to a drop of the heat transfer characteristic. For $N = 1$, j_h decreases when the fin spacing is increased. This phenomenon can be described from the flow field within the fin passage. From the numerical simulation (Torikoshi et al. [25]), the entire flow region can be kept laminar and steady and the vortex forms behind the tube can be suppressed for the tight fin. The cross-stream width

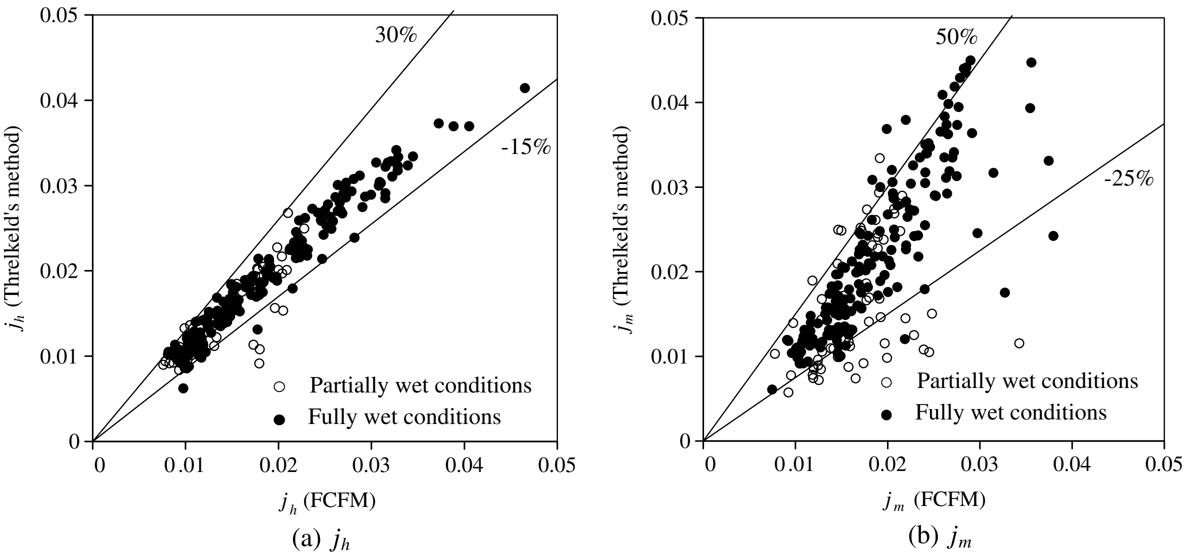

Fig. 4. Comparison between the data obtained from the present method and those obtained from the method of Threlkeld.

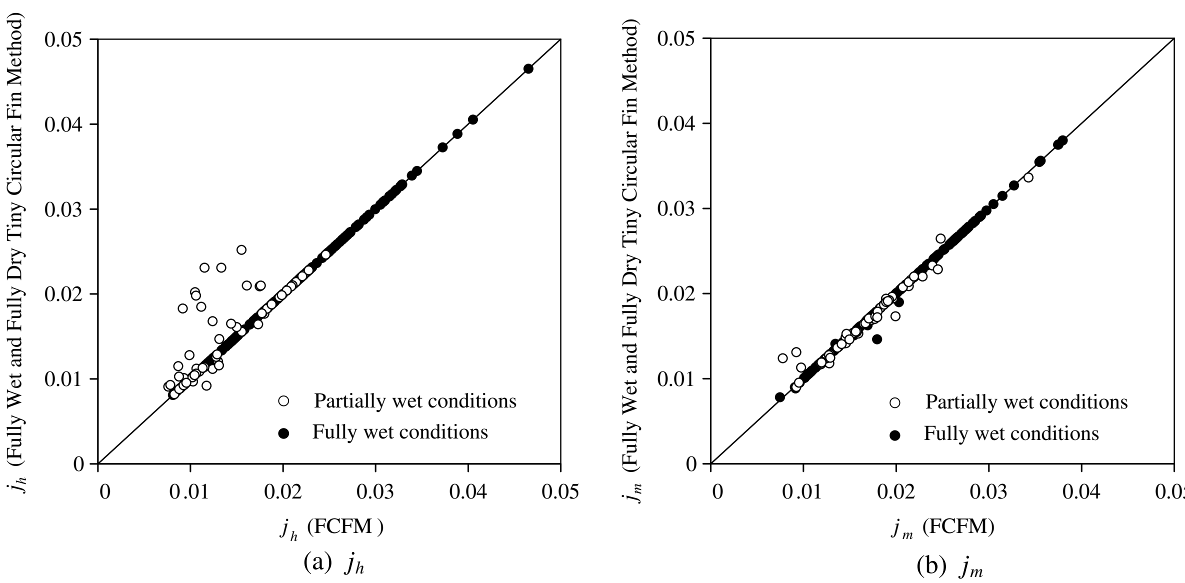

Fig. 5. Comparison between the data obtained from the present method and those obtained from the fully wet and fully dry tiny circular fin method (Pirompugd et al. [9,10]).

of the vortex region behind the tube will be taken place when the fin spacing increases. Then, the j_h decreases with the increasing of fin spacing for one-row configuration, indicating a detectable influence of fin spacing. The effect of fin spacing on j_h can be negligible when the number of tube rows is increased. This is because with the increasing number of tube row the subsequent row can block the condensate blow-off phenomenon from the preceding row. Moreover, when $N = 6$ and $RH = 50\%$, one can see the significant decline of j_h at low Re_{D_c}($Re_{D_c} < 2000$). This can be made clear from Fig. 6d, it shows that at a low inlet relative humidity most of the surface is actually dry for no condensation takes place. As a result, the outside surface is under the partially wet condition that leads to a drop of heat transfer characteristic.

Fig. 7a–d show the effects of inlet relative humidity and fin spacing on the j_m. The results indicate that the effect of inlet relative humidity on j_h is negligible when the fin spacing is larger than 2.5 mm,. However, for a smaller fin spacing, one can observe that the j_m increases when the inlet relative humidity is reduced from 90% to 50%. The decline of j_m for a tighter fin configuration can be attributed to the condensate retention phenomenon. As can be seen from the observation of flow patten conducted by Yoshii et al. [26], they had clearly indicated that the blockage of the tube row by the condensate retention when performing the experiment about the air flow across a tube bank. As a result, it may deteriorate the performance of the heat exchanger and show a slight drop in the j_m. However, a considerable rise of j_m is encountered when $RH = 0.5$ and

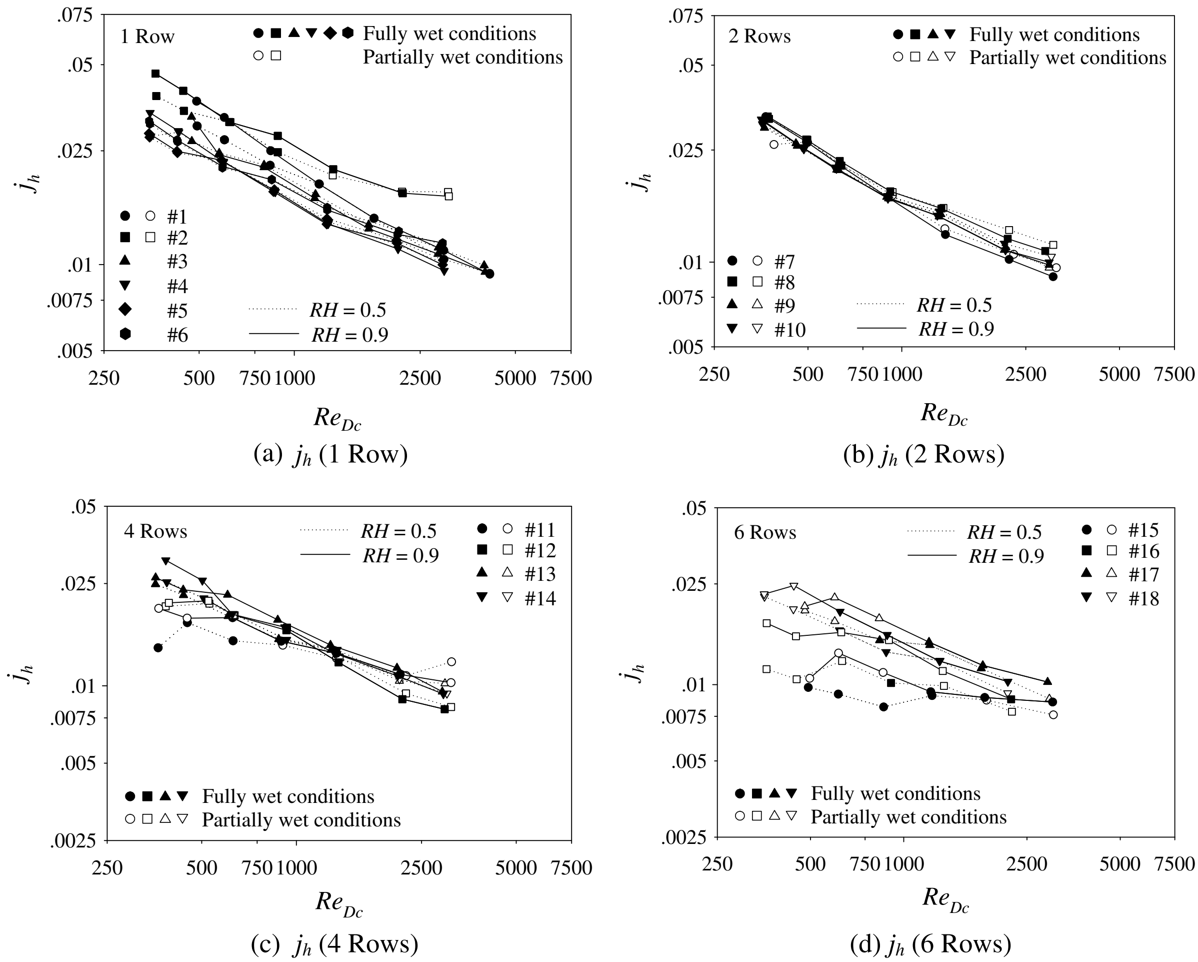

Fig. 6. j_h obtained from the present method.

$Re_{D_c} > 750$. This is related to the blow-off condensate caused by flow inertia, thereby making more room for condensation of water vapor to take place. Performance drop for j_h and j_m subject to influence of tube row can be made clear from Wang et al. [27]. They had conducted the flow visualization using scale-up fin-and-tube heat exchangers, showing that the incoming air first hits the first row tube and then, it twists and swirls to the subsequent row. The swirled motion is apparently stronger near the first row, and the strength of the swirled motion is reduced by the increase of tube row. The drop of swirled strength leads to an overall drop of heat/mass transfer performance with the number of tube row.

For the simultaneous heat and mass transfer, if mass transfer data are unavailable, one would resort to the analogy between the heat and mass transfer. For an air–water vapor mixture, the ratio of $h_{c,o}/h_{d,o}\ C_{p,a}$ is about unity. From the results of Seshimo et al. [28] and Eckels and Rabas [29], the corresponding values are about $1.1 \sim 1.2$. Hong and Webb [30] reported that this value is between $0.7 \sim 1.1$. In this study, the values of $h_{c,o}/h_{d,o}\ C_{p,a}$ are between 0.6 and 1.2. However, the present authors found that the results from the Threlkeld method did not entirely support the analogy between heat and mass transfer.

By using a multiple linear regression technique in a range of experimental data ($300 < Re_{D_c} < 5000$), the appropriate correlations of j_h and j_m based on the present data are as follows:

- $N = 1$ (fully wet and partially wet conditions)

$$j_{h,1} = 6.6412\left(\frac{P_l}{D_c}\right)^{-0.00085}\left(\frac{P_t}{D_c}\right)^{-2.1461} \times Re_{D_c}^{\left(-0.2636\frac{S_p}{D_c}-0.00091\frac{P_l}{D_c}+0.1558\frac{P_t}{D_c}-0.8865\right)} \quad (45)$$

$$j_{m,1} = 1.00006\left(\frac{P_l}{D_c}\right)^{-1.6741}\left(\frac{P_t}{D_c}\right)^{-0.6715} \times Re_{D_c}^{\left(-0.4252\frac{S_p}{D_c}+0.1398\frac{P_l}{D_c}+0.1408\frac{P_t}{D_c}-0.8472\right)} \quad (46)$$

$$R_1 = 0.9999\left(\frac{P_l}{D_c}\right)^{-0.3729}\left(\frac{P_t}{D_c}\right)^{1.7698} \times Re_{D_c}^{\left(0.1786\frac{S_p}{D_c}-0.00526\frac{P_l}{D_c}-0.1506\frac{P_t}{D_c}+0.1321\right)} \quad (47)$$

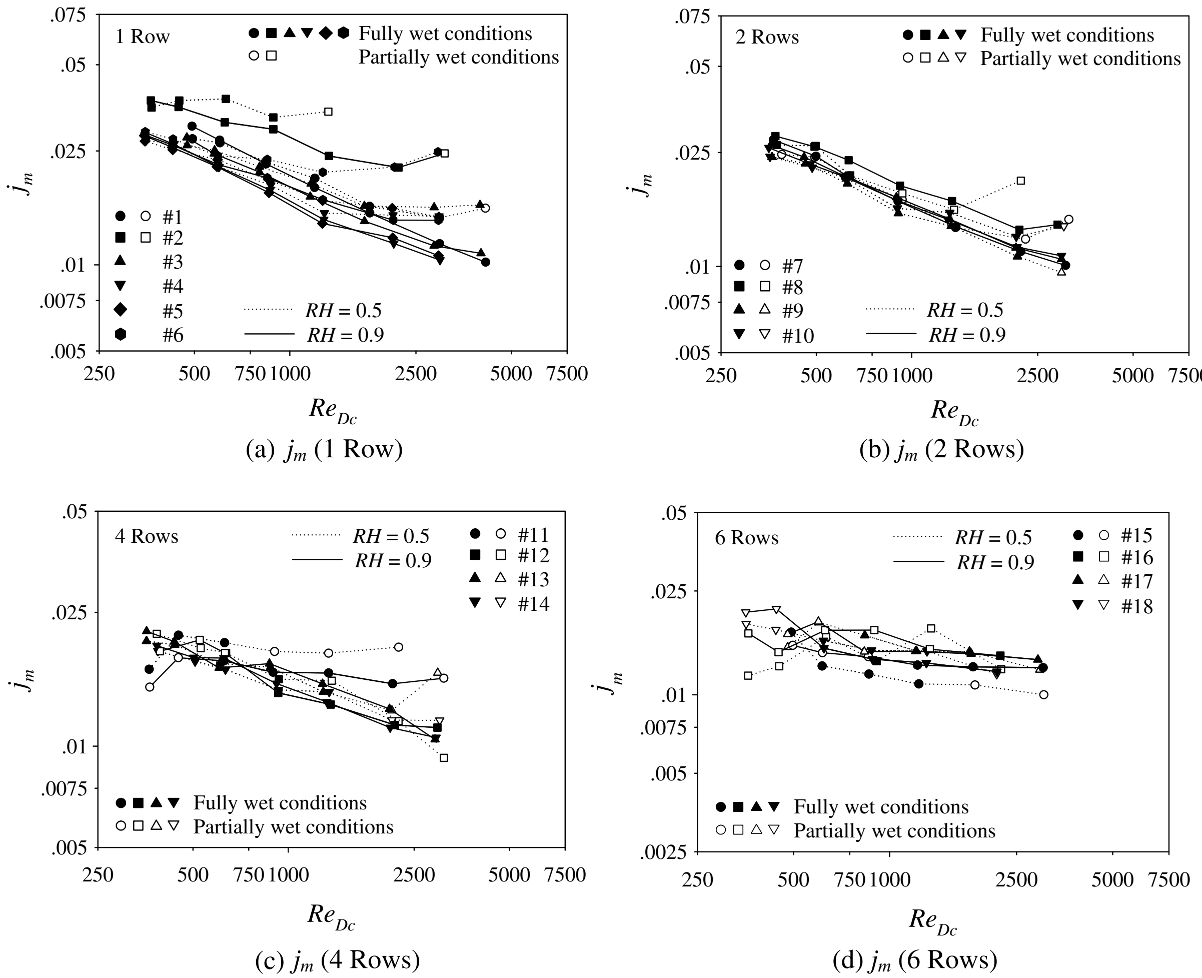

Fig. 7. j_m obtained from the present method.

- $N > 1$ (fully wet conditions)

$$j_{\mathrm{h},N,\mathrm{f}} = j_{\mathrm{h},1} N^{-0.06451} \left(\frac{S_\mathrm{p}}{D_\mathrm{c}}\right)^{(-0.1219N+0.7381)} \varepsilon^{(-0.1616N+0.6105)} \times Re_{D_\mathrm{c}}^{\left(0.03475N+0.1145\frac{S_\mathrm{p}}{D_\mathrm{c}}+0.00521\frac{P_\mathrm{l}}{D_\mathrm{c}}-0.03498\frac{P_\mathrm{t}}{D_\mathrm{c}}-0.04374\right)} \tag{48}$$

$$j_{\mathrm{m},N,\mathrm{f}} = j_{\mathrm{m},1} N^{0.1016} \left(\frac{S_\mathrm{p}}{D_\mathrm{c}}\right)^{(-0.2419N+2.5353)} \varepsilon^{(-0.312N+1.8373)} \times Re_{D_\mathrm{c}}^{\left(0.0654N-0.1935\frac{S_\mathrm{p}}{D_\mathrm{c}}+0.133\frac{P_\mathrm{l}}{D_\mathrm{c}}-0.2329\frac{P_\mathrm{t}}{D_\mathrm{c}}+0.1563\right)} \tag{49}$$

$$R_{N,\mathrm{f}} = R_1 N^{0.0272} \left(\frac{S_\mathrm{p}}{D_\mathrm{c}}\right)^{(0.1956N-1.9939)} \varepsilon^{(0.1616N-1.3425)} \times Re_{D_\mathrm{c}}^{\left(-0.0313N+0.2774\frac{S_\mathrm{p}}{D_\mathrm{c}}-0.1194\frac{P_\mathrm{l}}{D_\mathrm{c}}+0.1833\frac{P_\mathrm{t}}{D_\mathrm{c}}-0.1603\right)} \tag{50}$$

- $N > 1$ (partially wet conditions) (65% $A_\mathrm{wet}/A_\mathrm{o}$ 100 %)

$$j_{\mathrm{h},N,\mathrm{p}} = j_{\mathrm{h},N,\mathrm{f}} N^{-1.7838} \left(\frac{S_\mathrm{p}}{D_\mathrm{c}}\right)^{(-0.9459N+3.9329)} \left(\frac{A_\mathrm{wet}}{A_\mathrm{o}}\right)^{(0.6919N-4.7697)} \times Re_{D_\mathrm{c}}^{\left(-0.1554N+1.1667\frac{S_\mathrm{p}}{D_\mathrm{c}}+0.2253\frac{P_\mathrm{l}}{D_\mathrm{c}}-0.1645\frac{P_\mathrm{t}}{D_\mathrm{c}}+0.7158\right)} \tag{51}$$

$$j_{\mathrm{m},N,\mathrm{p}} = j_{\mathrm{m},N,\mathrm{f}} N^{-1.6415} \left(\frac{S_\mathrm{p}}{D_\mathrm{c}}\right)^{(-0.7655N+4.0144)} \left(\frac{A_\mathrm{wet}}{A_\mathrm{o}}\right)^{(1.16N-7.793)} \times Re_{D_\mathrm{c}}^{\left(-0.1151N+0.695\frac{S_\mathrm{p}}{D_\mathrm{c}}+0.5492\frac{P_\mathrm{l}}{D_\mathrm{c}}-0.4798\frac{P_\mathrm{t}}{D_\mathrm{c}}+0.974\right)} \tag{52}$$

$$R_{N,\mathrm{p}} = R_{N,\mathrm{f}} N^{-0.844} \left(\frac{S_\mathrm{p}}{D_\mathrm{c}}\right)^{(0.3364N-2.7278)} \left(\frac{A_\mathrm{wet}}{A_\mathrm{o}}\right)^{(-0.8774N+4.801)} \times Re_{D_\mathrm{c}}^{\left(0.0891N+0.5103\frac{S_\mathrm{p}}{D_\mathrm{c}}-0.3863\frac{P_\mathrm{l}}{D_\mathrm{c}}+0.3393\frac{P_\mathrm{t}}{D_\mathrm{c}}-0.7031\right)} \tag{53}$$

Detailed comparisons of the proposed correlations against the experimental data are shown in Fig. 8a–c. It is found that Eqs. (45), (48) and (51) can describe 95.63% of j_h within 15%, Eqs. (46), (49) and (52) can describe 95.14% of j_m

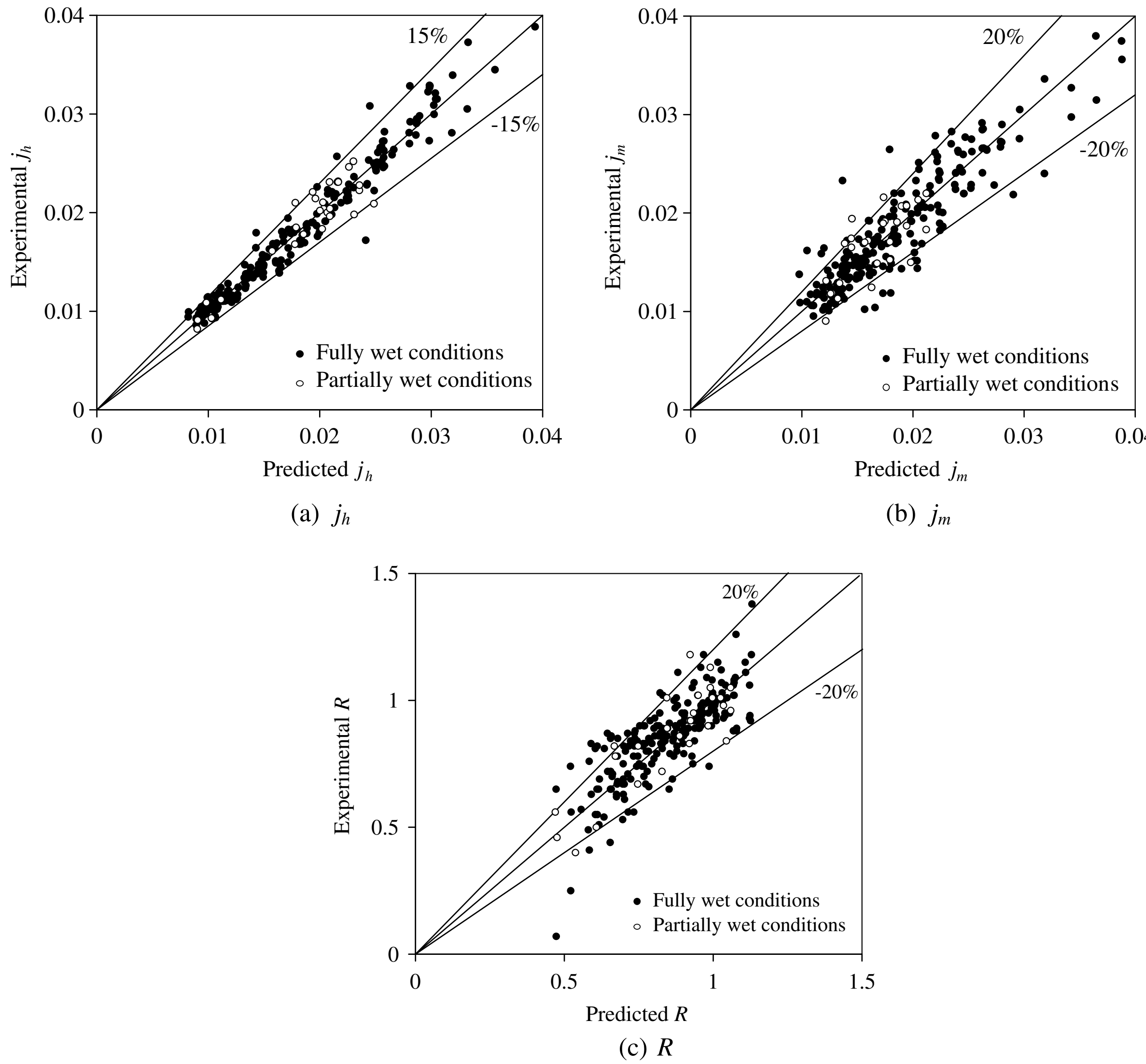

Fig. 8. Comparison between predicted data and experimental data.

within 20% and Eqs. (47), (50) and (53) can describe 94.68% of $h_{c,o}/h_{d,o}C_{p,a}$ within 20%.

5. Conclusions

This study proposes a new reduction method to analyze the heat and mass transfer characteristic of the experimentally data from 17 wavy fin-and-tube heat exchangers under dehumidifying conditions. On the basis of previous discussions, the following conclusions are made:

1. A reduction method that is capable of handling fully wet, fully dry, and partially wet surface is proposed in this study. It is found that the proposed method is superior to previous method.
2. The heat transfer and mass transfer characteristics obtained by the present method are relatively insensitive to the inlet relative humidity. However, the effect of relative humidity on the mass transfer characteristic becomes more pronounced when partially wet condition takes place.
3. The heat transfer characteristic is comparatively independent of the fin spacing. Effect of fin spacing on the mass transfer characteristic is rather small when fin spacing is larger than 2.5 mm. However, at a smaller fin spacing, j_m slightly decreases when the relative humidity increases.
4. The correlations applicable to the present wavy fin-and-tube heat exchanger are proposed. These correlations can describe 95.63% of j_h within ±15%, can describe 95.14% of j_m within ±20% and can describe 94.68% of R within ±20%.

Acknowledgments

The authors are indebted to the Thailand Research Fund (TRF) and the funding from Department of Industrial Technology of the Ministry of Economic Affairs, Taiwan for supporting this study.

References

[1] D.T. Beecher, T.J. Fagan, Effects of fin pattern on the air side heat transfer coefficient in plate finned-tube heat exchanger, ASHRAE Trans. 93 (2) (1987) 1961–1984.

[2] W.M. Yan, P.J. Sheen, Heat transfer and friction characteristics of fin-and-tube heat exchangers, Int. J. Heat Mass Transfer 43 (2000) 1651–1659.

[3] C.C. Wang, W.L. Fu, C.T. Chang, Heat transfer and friction characteristics of typical wavy fin-and-tube heat exchangers, Exp. Therm. Fluid Sci. 14 (2) (1997) 174–186.

[4] C.C. Wang, Y.M. Tsi, D.C. Lu, Comprehensive study of convex-louver and wavy fin-and-tube heat exchangers, AIAA J. Thermophys. 12 (3) (1998) 423–430.

[5] C.C. Wang, Y.T. Lin, C.J. Lee, Investigation of wavy fin-and-tube heat exchangers: a contribution to data bank, Exp. Heat Transfer 12 (1999) 73–89.

[6] C.C. Wang, Y.M. Hwang, Y.T. Lin, Empirical correlations for heat transfer and flow friction characteristics of herringbone wavy fin-and-tube heat exchangers, Int. J. Refrig. 25 (2002) 673–680.

[7] Y.T. Lin, Y.M. Hwang, C.C. Wang, Performance of the herringbone wavy fin under dehumidifying conditions, Int. J. Heat Mass Transfer 45 (2002) 5035–5044.

[8] W. Pirompugd, S. Wongwises, C.C. Wang, Simultaneous heat and mass transfer characteristics for wavy fin-and-tube heat exchangers under dehumidifying conditions, Int. J. Heat Mass Transfer 49 (1–2) (2006) 132–143.

[9] W. Pirompugd, C.C. Wang, S. Wongwises, Heat and mass transfer characteristics for finned tube heat exchangers with humidification, J. Thermophys. Heat Transfer 21 (2) (2007) 361–371.

[10] W. Pirompugd, C.C. Wang, S. Wongwises, A fully wet and fully dry tiny circular fin method for heat and mass transfer characteristics for plain fin-and-tube heat exchangers under dehumidifying conditions, J. Heat Transfer 129 (9) (2007) 1256–1267.

[11] Y. Xia, A.M. Jacobi, Air side data interpretation and performance analysis for heat exchangers with simultaneous heat and mass transfer: wet and frosted surfaces, Int. J. Heat Mass Transfer 48 (2005) 5089–5102.

[12] W. Pirompugd, C.C. Wang, S. Wongwises, Finite circular fin method for heat and mass transfer characteristics for plain fin-and-tube heat exchangers under fully and partially wet surface conditions, Int. J. Heat Mass Transfer 50 (3–4) (2007) 552–565.

[13] ASHRAE Standard 41.2-1987, Standard methods for laboratory air-flow measurement. American Society of Heating, Refrigerating and Air-Conditioning Engineers, Inc., Atlanta GA, 1987.

[14] ASHRAE Standard 41.1-1986, Standard method for temperature measurement. American Society of Heating, Refrigerating and Air-Conditioning Engineers, Inc., Atlanta, GA, 1986.

[15] ASHRAE Standard 2000, Method of testing forced circulation air cooling and air heating coils. American Society of Heating, Refrigerating and Air-Conditioning Engineers, Inc., Atlanta, GA, 2000, pp. 33–78.

[16] R.J. Moffat, Describing the uncertainties in experimental results, Exp. Therm. Fluid Sci. 1 (1988) 3–17.

[17] T.R. Bump, Average temperatures in simple heat exchangers, ASME J. Heat Transfer 85 (2) (1963) 182–183.

[18] R.J. Myers, The effect of dehumidification on the air-side heat transfer coefficient for a finned-tube coil, M.S. Thesis, University of Minnesota, Minneapolis, 1967.

[19] J.L. Threlkeld, Thermal Environmental Engineering, Prentice-Hall, Inc., NY, 1970.

[20] V. Gnielinski, New equation for heat and mass transfer in turbulent pipe and channel flow, Int. Chem. Eng. 16 (1976) 359–368.

[21] C.C. Wang, Y.C. Hsieh, Y.T. Lin, Performance of plate finned tube heat exchangers under dehumidifying conditions, J. Heat Transfer 119 (1997) 109–117.

[22] S.G. Kandlikar, Thermal design theory for compact evaporators, in: R.K. Shah, A.D. Kraus, D. Metzger (Eds.), Compact Heat Exchangers – A Festschrift for A.L. London, Hemisphere Publishing Corp., NY, 1990, pp. 245–286.

[23] W. Pirompugd, S. Wongwises, C.C. Wang, A tube-by-tube reduction method for simultaneous heat and mass transfer characteristics for plain fin-and-tube heat exchangers in dehumidifying conditions, Heat Mass Transfer 41 (8) (2005) 756–765.

[24] D.Q. Kern, A.D. Kraus, Extended Surface Heat Transfer, 1972, pp. 102–106.

[25] K. Torikoshi, G. Xi, Y. Nakazawa, H. Asano, Flow and heat transfer performance of a plate-fin and tube heat exchanger (1st report: effect of fin pitch), in: Tenth International Heat and Transfer Conference 1994 Paper 9-HE-16, 1994, pp. 411–416.

[26] T. Yoshii, M. Yamamoto, M. Otaki, Effects of dropwise condensate on wet surface heat transfer of air cooling coils, in: Proceedings of the 13th International Congress of Refrigeration, 1973, pp. 285–292.

[27] C.C. Wang, J. Lo, Y.T. Lin, C.S. Wei, Flow visualization of annular and delta winglet vortex generators in fin-and-tube heat exchanger application, Int. J. Heat Mass Transfer 45 (2002) 3803–3815.

[28] Y. Seshimo, K. Ogawa, K. Marumoto, M. Fujii, Heat and mass transfer performances on plate fin-and-tube heat exchangers with dehumidification, Trans. JSME 54 (499) (1988) 716–721.

[29] P.W. Eckels, T.J. Rabas, Dehumidification on the correlation of wet and dry transport process in plate finned-tube heat exchangers, ASME J. Heat Transfer 109 (1987) 575–582.

[30] T.K. Hong, R.L. Webb, Calculation of fin efficiency for wet and dry fins, Int. J. HVAC & R Research 2 (1) (1996) 27–41.